FREE VIBRATION OF KINKED CANTILEVER WITH ATTACHED MASSES

B. S. REDDY, K. R. Y. SIMHA AND A. GHOSAL
Department of Mechanical Engineering
Indian Institute of Science
India

Abstract

This paper analyses free vibration characteristics of a centrally kinked cantilever beam of unit mass carrying masses at the kink (m_k) and at the tip (m_t). Frequency factors are presented for the first two modes for different combinations of m_k,m_t and the kink angle δ. A relationship of the form $f(m_k, m_t, \delta) = m_k + m_t(4 + \frac{10}{3}\cos\delta + \frac{2}{3}\cos^2\delta) = \mathit{constant}$ appears to give the same fundamental frequency for a given δ and different combinations of $[m_k, m_t]$. Mode shapes as well as bending moments at the support and at the kink are also discussed. The utility of a discrete beam model in understanding the free vibration characteristics is also highlighted.

Notation

m_k = nondimensional kink mass
m_t = nondimensional tip mass
m_{ek} = effective kink mass
m_{et} = effective tip mass
M_k = bending moment at kink
M_s = bending moment at support
δ = kink angle
w = bending displacement
w_t = tip displacement
w_k = kink displacement
EI = flexural rigidity
E = Young's modulus
I = moment of inertia
ρ = mass density of beam
A = area of beam cross section
L = beam length
$K = [\omega_j^2 \rho A/EI]^{\frac{1}{4}}$
$y_j = (KL)_j$ = eigenvalue of j th mode of vibration
C_j = mode shape constants
ω_j = frequency

p_j = frequency factor
$\hat{M}_{stat}$ = static moment at support per unit tip deflection
$\hat{M}_{dyn}$ = dynamic moment at support per unit tip deflection
$D_s = \hat{M}_{dyn}/\hat{M}_{stat}$ at support
$D_k = M_k/M_s$
F = flexibility matrix
K_s = stiffness matrix
M = mass matrix
α = mass ratio $(\frac{m_{ek}}{m_{et}})$

1 Introduction

Free vibration of cantilevers carrying discrete masses along their length constitutes a fundamental problem in acoustics, seismology, flexible manipulators and a variety of other engineering applications. This classical problem has been approached at different levels of approximation ranging from the simplest discrete model of a massless beam with flexural rigidity to Timoshenko models which take into account shear deformation as well as rotary inertia [1]. Extensive work has been done using the massless beam formulation for analyzing the seismic response of multistoried buildings [2,3]. Similarly, a large amount of results are also available for straight beams with only a tip mass [4,5] or a system of masses [6]. Continuous beam formulation for a kinked cantilever carrying a tip mass and central mass using Euler - Bernoulli theory appears not to have been studied analytically. One of the reasons for this lacuna might be the explosive growth of numerical methods for vibration and modal analysis in the past few decades. Notwithstanding this situation, it is important to extend analytical methods to gain better insight for engineering design.

A kinked cantilever beam, as shown in Figure 1, is a viable model of a two link flexible manipulator with m_k representing a motor and m_t the payload. In flexible manipulators with rotary joints, the joints permit free rotation of link during the motion of the payload, however, the rotations at the joints are stopped by control (actuator) torques once the payload reaches a desired destination. This maneuver typically induces vibrations in the flexible manipulator and suppression of unwanted vibration is an important problem in flexible manipulators [7]. The two link manipulator can be modeled as a single cantilever with a kink of some angle δ with the torques M_k and M_s representing the bending moments at the kink and support, respectively. Another example of a kinked cantilever situation arises in plastic bending under impact at the kink [8]. The resulting response after the kink formation is the free vibration of a kinked elastic beam. In addition, attaching masses to reduce noise and vibration levels have been widely used for beams, plates and shells [9]. Although the emphasis in vibration engineering is on reducing acoustic radiation, it is important to understand the dynamic stress levels during free or forced vibration. Hence, understanding free vibration characteristics of a kinked cantilever carrying masses can help

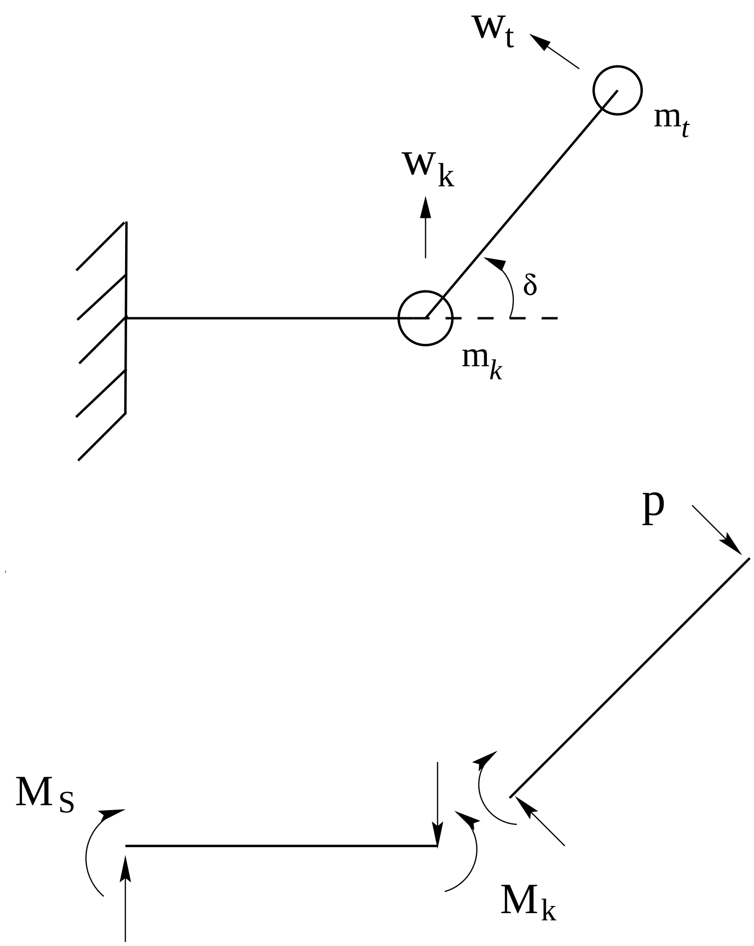

Figure 1: A Kinked Cantilever

in evolving better active or passive control schemes in the case of flexible manipulators, better design procedures in impact engineering or reducing acoustic radiation.

This paper deals with the effect of varying tip mass and the central mass on free vibration characteristics of a kinked cantilever beam. Non-dimensional design factors for the natural frequencies, mode shapes and bending moments are provided in the form of tables, charts and graphs for ready reference to the designer. Analytical results derived in this paper are verified using a commercial FEM software package. This paper is arranged as follows: Section 2 presents the mathematical formulation of expressions for the frequencies, mode shapes and the bending moments of a kinked beam. Section 3 describes, in brief, the FE model used to validate the analytical results. Section 4 presents and discusses the numerical results obtained from analytical and FE models. The results of the analytical model appear to be in general agreement with the FEM results but they deviate for large kink angles. A relationship in the form $f(m_k, m_t, \delta) = m_k + m_t(4 + \frac{10}{3}\cos\delta + \frac{2}{3}\cos^2\delta) = constant$ appears to give the same fundamental frequency for a given δ and different combinations of m_k and m_t. Section 5 presents the conclusions of this paper.

2 Mathematical Formulation

The free vibration of a cantilever beam is governed by the well-known partial differential equation

$$EI\frac{\partial^4 w}{\partial x^4} + \rho A\frac{\partial^2 w}{\partial t^2} = 0. \tag{1}$$

where w is the transverse deflection, EI is flexural rigidity, ρ is mass density and A is cross sectional area.

The above partial differential equation can be solved by the well known technique of separation of variables. For a kinked cantilever of total length L, we consider a solution of the form $w_i(x,t) = X_i(x)T(t)$ where $i = 1, 2$, denotes the two halves of the beam. The mode shapes X_1 and X_2 for the two halves of the beam are of the form

$$\begin{aligned} X_1 &= C_1\cos(Kx) + C_2\sin(Kx) + C_3\cosh(Kx) + C_4\sinh(Kx) \\ X_2 &= C_5\cos(Kx) + C_6\sin(Kx) + C_7\cosh(Kx) + C_8\sinh(Kx) \end{aligned} \tag{2}$$

where $K^4 = \frac{\omega_j^2\rho A}{EI}$.

The boundary conditions to determine the constants C_j are as follows.

At the fixed support,

$$w_1 = w_1' = 0 \tag{3}$$

The bending displacement continuity at the kink stipulates

$$w_1\cos\delta = w_2 \tag{4}$$

The shear force balance at the kink, taking an effective mass of $m_k + (m_t + 1/2)\sin\delta$, gives

$$EI(w_1''' - w_2'''\cos\delta) = [m_k + (m_t + 1/2)\sin\delta]\ddot{w}_1 \tag{5}$$

At the kink, the continuity of slope and bending moment requires

$$\begin{aligned} w_1' &= w_2' \\ w_1'' &= w_2'' \end{aligned} \tag{6}$$

Finally, at the free end

$$\begin{aligned} w_2'' &= 0 \\ EIw_2''' &= m_t\ddot{w}_2. \end{aligned} \tag{7}$$

In the above equations $()'$ and $\ddot{()}$ denote derivatives with respect to x and t respectively. Thus, there are two boundary conditions at both the free end and the fixed end, and four conditions at the kink giving a total of 8 equations for 8 unknown coefficients C_j. Substitution of assumed solutions (2) in the boundary conditions lead to the eigen equation

$$F(KL)[C_1.....C_8]^T = 0. \tag{8}$$

where $F(KL)$ is an 8x8 matrix whose elements are given in the Appendix. For non-trivial solutions, $\det(F) = 0$ gives the equation for the natural frequencies as a function of m_k, m_t and δ. The roots of this equation give positive values of KL which are used to obtain the frequencies and the coefficients C_j. The eigenvalue $y_j = KL$ is related to the frequency ω_j by

$$\omega_j = (\frac{y_j}{L})^2\sqrt{\frac{EI}{\rho A}} \tag{9}$$

The equations (8) and (9) were solved numerically for various sets of values of m_k, m_t and δ and these results are presented and discussed in detail in section 4. A frequency factor, p_j, is helpful in presenting the results and is defined as the ratio of the frequency of a kinked beam for a given (m_k, m_t, δ) to the frequency of a straight beam with no attached masses. For mode 1 (j=1) and mode 2 (j=2), p_j is given by

$$p_j = \frac{\omega_j(m_k, m_t, \delta)}{\omega_j(0, 0, 0)} \tag{10}$$

2.1 Bending Moments

The bending moments of the kinked cantilever beam can be obtained from the Euler-Bernoulli beam theory. At the mid-point of the kinked beam, $x = L/2$, the moment at the kink in terms of $y = KL$ is given by

$$M_k = \frac{EIy^2}{L^2}[-C_1 \cos\frac{y}{2} - C_2 \sin\frac{y}{2} + C_3 \cosh\frac{y}{2} + C_4 \sinh\frac{y}{2}] \tag{11}$$

At the support, $x = 0$, the moment is given by $M_s = -2EIC_1y^2/L^2$. The ratio of the moments at the kink and support, denoted by D_k, is given by

$$D_k = \frac{M_k}{M_s} = \frac{1}{2}[\cos\frac{y}{2} + \frac{C_2}{C_1}\sin\frac{y}{2} - \frac{C_3}{C_1}\cosh\frac{y}{2} - \frac{C_4}{C_1}\sinh\frac{y}{2}] \tag{12}$$

The dynamic bending moment normalized with respect to a unit tip deflection is

$$\hat{M}_{dyn} = \frac{EIX''(0)}{X_2(L)} \tag{13}$$

In order to compare the dynamic bending moment with the static situation, a static load P at the tip is considered (see figure 1). In the static case the bending moment at the support is given as

$$M_{stat} = \frac{PL}{2}(1 + \cos\delta) \tag{14}$$

The corresponding tip deflection is given by

$$\frac{PL^3}{24EI}[4 + 3\cos\delta + \cos^2\delta] \tag{15}$$

Hence, the bending moment per unit tip deflection is given by

$$\hat{M}_{stat} = \frac{3EI}{L^2}\frac{4(1+\cos\delta)}{4 + 3\cos\delta + \cos^2\delta} \tag{16}$$

For the straight beam with $\delta = 0$, $\hat{M}_{stat} = 3EI/L^2$. It is useful to define the ratio of $\hat{M}_{dyn}$ to $\hat{M}_{stat}$ for a straight beam as D_s, given by

$$D_s = \frac{\hat{M}_{dyn}}{3(\frac{EI}{L^2})} \tag{17}$$

It may be noted that $\hat{M}_{stat}$ is zero for $\delta = \pi$ (see equation 16).

The quantity D_k is the ratio of bending moment at the kink to that at the support under dynamic condition. Thus the dynamic bending moment factors D_s and D_k provide the amplification in bending moments due to free vibrations. In section 4, numerical values of bending moments and the ratios discussed above are presented for various values of m_k, m_t and δ.

2.2 Discrete Analysis of the Kinked Beam

A discrete model of a continuous system often helps in understanding the dynamic characteristics with regard to frequencies, displacements and moments. In this section, a discrete model, with the beam assumed to be massless, is derived. The discrete model gives inaccurate results for small values of m_k and m_t, however, it is shown that the discrete element model predicts many important features of the continuous kinked beam system.

Assuming that E, I and L are unity, the flexibility matrix of a discrete kinked beam is given by

$$F = \frac{1}{48}\begin{bmatrix} 2 & 3 + 2\cos\delta \\ 3 + 2\cos\delta & 8 + 6\cos\delta + 2\cos^2\delta \end{bmatrix};$$

The stiffness and mass matrice are given as

$$\begin{aligned} K_s &= F^{-1} \\ M &= \begin{bmatrix} m_{ek} & 0 \\ 0 & m_{et} \end{bmatrix} \end{aligned} \tag{18}$$

where $m_{ek} = m_k + m_t \sin\delta$; $m_{et} = m_t$. Expanding $|K_s - M\omega^2| = 0$ gives the frequency equation

$$\omega^4 - (\frac{96}{7})(\frac{1}{m_{et}} + \frac{4 + 3\cos\delta + \cos^2\delta}{m_{ek}})\omega^2 + \frac{48^2}{7}\frac{1}{m_{ek}m_{et}} = 0$$

From the above equation, we conclude that the product of $\omega_1^2\omega_2^2$ is invariant with respect to the product $m_{ek}m_{et}$. Defining a mass ratio $\alpha = \frac{m_{ek}}{m_{et}}$ the individual values of ω_1^2, ω_2^2 are

$$\omega_{1,2}^2 = \frac{48}{7m_{ek}}[(\alpha + 4 + 3\cos\delta + \cos^2\delta) \pm \sqrt{(\alpha + 4 + 3\cos\delta + \cos^2\delta)^2 - 7\alpha}\ ] \tag{19}$$

The fundamental frequency is given by,

$$\omega_1^2 = \frac{48}{7m_{ek}}(\alpha + 4 + 3\cos\delta + \cos^2\delta)[1 - \sqrt{1 - \frac{7\alpha}{(\alpha + 4 + 3\cos\delta + \cos^2\delta)^2}}\ ] \tag{20}$$

Assuming $\frac{7\alpha}{(\alpha+4+3\cos\delta+\cos^2\delta)^2} << 1$, we get

$$\omega_1^2 = \frac{24}{m_{ek} + m_{et}(4 + 3\cos\delta + \cos^2\delta)} \tag{21}$$

The above result implies that the fundamental frequency will not change if $m_{ek} + m_{et}(4 + 3\cos\delta + \cos^2\delta)$ is held constant. Recalling that $m_{ek} = m_k + m_t \sin\delta$ and $m_{et} = m_t$, the condition yields $m_k + m_t(4 + 3\cos\delta + \sin\delta + \cos^2\delta) = C$, a constant, for constant fundamental frequency. As an example, when $\delta = 0$, the iso-frequency locus of ω_1 in the $m_k - m_t$ plane is a straight line $m_k + 8m_t = C$. Figure 2 shows the ω_1 locus for $C = 20$. In the same figure ω_2 and $\omega_1\omega_2$ loci are also shown with all the loci passing through $(2, 4)$ and $(16, 0.5)$ in the $m_k - m_t$ plane. These observations are useful in discussing the frequency results for the continuous kinked beam presented in Section 4.

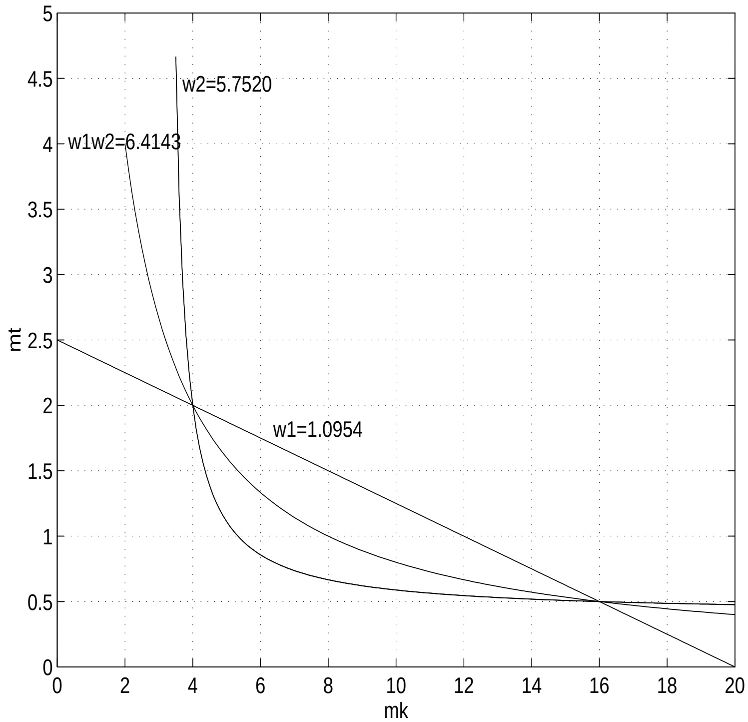

Figure 2: Variations of ω_1, ω_2 and $\omega_1\omega_2$ with m_k and m_t

The ratio of tip displacement to kink displacement in the fundamental mode is only a function of α

$$\frac{\delta_t}{\delta_k} = \frac{256 + 25\alpha}{80 + 10\alpha};$$

The bending moment at the support per unit tip deflection in the fundamental mode also depends only on α.

$$\frac{M_s}{\delta_t} = 24(\frac{\alpha+8}{7})(\frac{5}{16 - [(\alpha+8)(1-\sqrt{(1-\frac{7\alpha}{(\alpha+8)^2})})]} + \frac{2}{\alpha})(1-\sqrt{(1-\frac{7\alpha}{(\alpha+8)^2})}) \tag{22}$$

3 Finite Element Analysis

In order to assess the validity of the results obtained using the Euler-Bernoulli beam model, a FE analysis was undertaken. The beam is modeled using four 2-D beam elements as shown in figure 3 which also shows a typical beam element. Each element has two nodes and each node has 3 degrees of freedom so that it can translate in X and Y directions and rotate in XY plane. For the node at the fixed end all the degrees of freedom are arrested. A mass element is attached at the tip and at the kink. A commercial FEM package NISA is used to solve the eigenvalue problem using a conventional, subspace iteration method for fixed values of E, I, A, L and for different combinations of m_k, m_t and δ. Results for the frequencies, and mode shapes, and comparison of the FEM results with the analytical results are discussed in section 4.

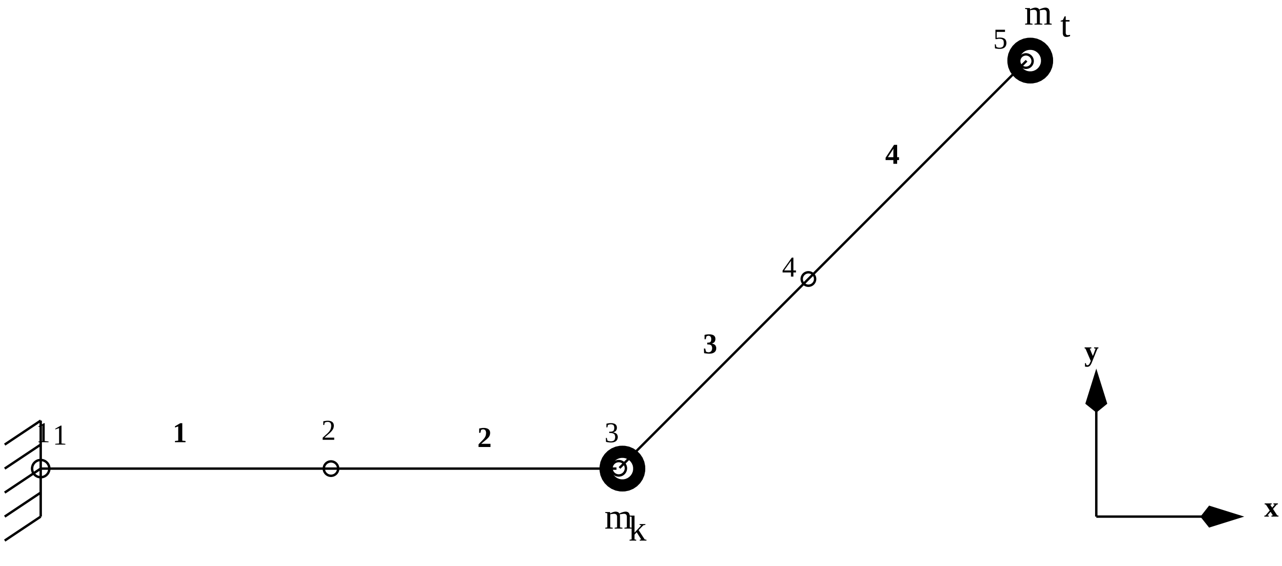

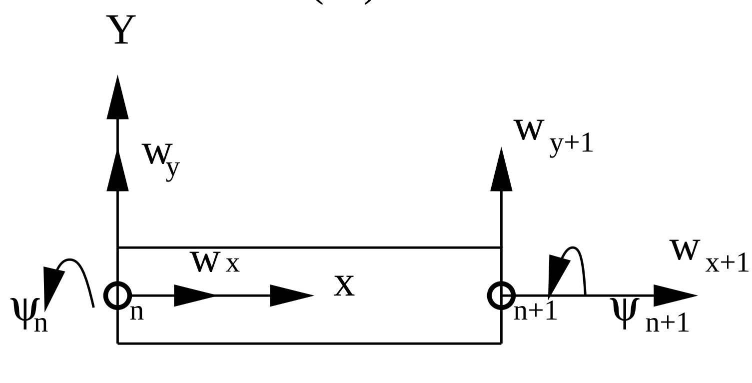

Figure 3: (a) FEM model of kinked beam (b) A typical element of the model

4 Results and Discussion

In this section, results related to the natural frequencies, mode shapes and bending moments in a kinked cantilever with masses attached at the kink and free end are presented and discussed. Only the effect of m_k, m_t and δ on the free vibration characteristics are considered although E, I, L also affect the free vibration characteristics.

Frequency Analysis

To obtain frequency factors, equation (8) was solved numerically using the software package Matlab [10] and KL was obtained for various values of m_k, m_t and δ. Once KL is known, the frequency ω_j and the frequency factor p_j is obtained from equations (9) and (10) respectively. The FEM results, as mentioned before, were obtained from NISA.

Frequency factors and the FEM results are tabulated in Table 1 for the first two modes for different combinations of m_k, m_t and δ. As the values of attached masses increase, the frequency factors drop as seen in Table 1. It can be also seen from figures 4 and 5, that as the kink angle increase the frequency factors increase in mode 1 and decrease in mode 2 for a given combination of m_k and m_t. It may be noted that the fundamental frequency increases roughly 3 times as the kink angle increases from 0 to π. For a 90° kink, the increase in fundamental frequency is about 30% from its value for a straight beam. Thus, the kink effect becomes more pronounced after 90°.

It may be noted that the FEM and analytical results in Table 1 are in good agreement except at large kink angles for some combinations of m_k and m_t. A possible reason for this discrepancy could be that in the FEM model the nodes were allowed to translate in axial direction and hence axial vibration is not arrested. Regarding the mode 2 frequency factors displayed in figure 5, there is an unexplained deviation in the trend for $m_k = 0, m_t = 1$ around $\delta = 150°$. This combination of m_k, m_t and δ also results in large unexplained values for mode shape coefficients in Table 2.

For a given kink angle it is possible to find an infinite number of m_k and m_t combinations that give the same fundamental frequency. These combinations appear to fit the equation $m_k + m_t(4 + \frac{10}{3}\cos\delta + \frac{2}{3}\cos^2\delta) = constant$. This result was obtained after trial and error and was motivated by the discrete beam analysis presented in section 2 which shows that $m_k + [4 + 3\cos\delta + \cos^2\delta + \sin\delta]m_t = constant$. It may be noted that the expression inside the bracket, $(4 + \frac{10}{3}\cos\delta + \frac{2}{3}\cos^2\delta)$, is equal to 8 when $\delta = 0$ as required by the discrete model. It should, however, be noted that the above fit is not accurate for low values of m_k and m_t, or for high kink angles. For a hairpin like kinked beam, e.g. $\delta = 175°$, the loci of iso-frequency points are curved as shown in figure 6. For smaller kink angles the loci are nearly straight as shown in figure 7.

Mode Shapes

The solution of equation (8) also yields $C_j,\ j = 1, ..., 8$ which determine the mode shapes for the kinked cantilever. The mode shapes for $m_k = m_t = 0$ for different kink angles are presented in figures 8 and 9. The mode shapes for $m_k = m_t = 1$ for different kink angles are shown in figures 10 and 11.

Mode shape coefficients for various sets of m_k and m_t for the first two modes are given in Tables 2 and 3. It is possible to use this information to construct the mode shapes for all the combinations of m_k, m_t and δ by means of interpolation. Table 2 applies for the first mode of vibration in which both segments of the kinked beam bend in the same direction. Table 3 applies for the second mode of vibration where the two segments bend in opposite directions. This is

Table 1: FREQUENCY FACTORS FOR KINKED BEAM

			MODE 1	MODE 1	MODE 2	MODE 2
m_k	m_t	δ	ANALYTICAL	FEM	ANALYTICAL	FEM
0	0	0^o	1.0000	1.0000	1.0000	1.0000
0	1	-	0.4430	0.4449	0.7375	0.7539
1	1	-	0.4256	0.4276	0.4297	0.4437
8	1	-	0.3380	0.3397	0.2235	0.2317
80	10	-	0.1128	0.1134	0.0727	0.0755
0	0	30^o	1	1.0299	0.8149	0.8674
0	1	-	0.4432	0.4577	0.4592	0.511
1	1	-	0.4318	0.4348	0.3485	0.3790
8	1	-	0.3409	0.3433	0.2142	0.2206
80	10	-	0.1134	0.1144	0.0708	0.0728
0	0	60^o	1.1136	1.1271	0.6897	0.6977
0	1	-	0.5000	0.5012	0.3557	0.3658
1	1	-	0.4773	0.4772	0.2922	0.2998
8	1	-	0.3636	0.3627	0.1978	0.2018
80	10	-	0.1136	0.1144	0.0653	0.0660
0	0	90^o	1.3295	1.3159	0.5789	0.5808
0	1	-	0.5909	0.5859	0.2922	0.2942
1	1	-	0.5455	0.5504	0.2450	0.2489
8	1	-	0.3864	0.3891	0.1815	0.1854
80	10	-	0.1250	0.1259	0.0599	0.0603
0	0	150^o	2.0114	2.2520	0.4537	0.4733
0	1	-	0.8636	0.8788	0.2577	0.3187
1	1	-	0.7955	0.8010	0.1960	0.2169
8	1	-	0.4545	0.4577	0.1615	0.1659
80	10	-	0.1477	0.1488	0.0544	0.0547
0	0	175^o	2.5909	2.6777	0.4483	0.4620
0	1	-	0.9205	0.9303	0.3721	0.4469
1	1	-	0.8750	0.8811	0.2105	0.2244
8	1	-	0.4773	0.4806	0.1597	0.1659
80	10	-	0.1477	0.1488	0.0544	0.0547

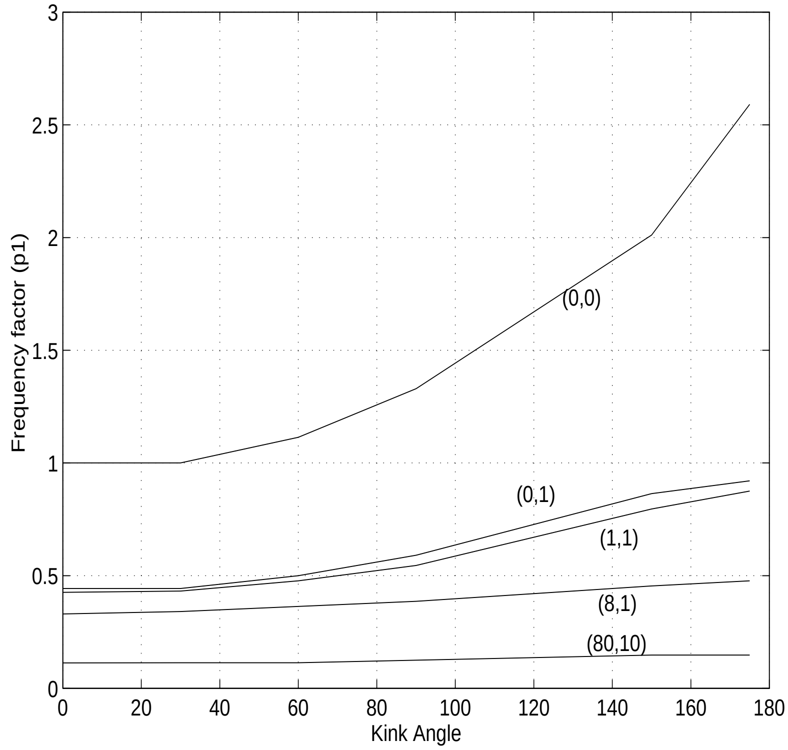

Figure 4: Mode 1 frequency factor vs Kink angle (δ) for different (m_k, m_t)

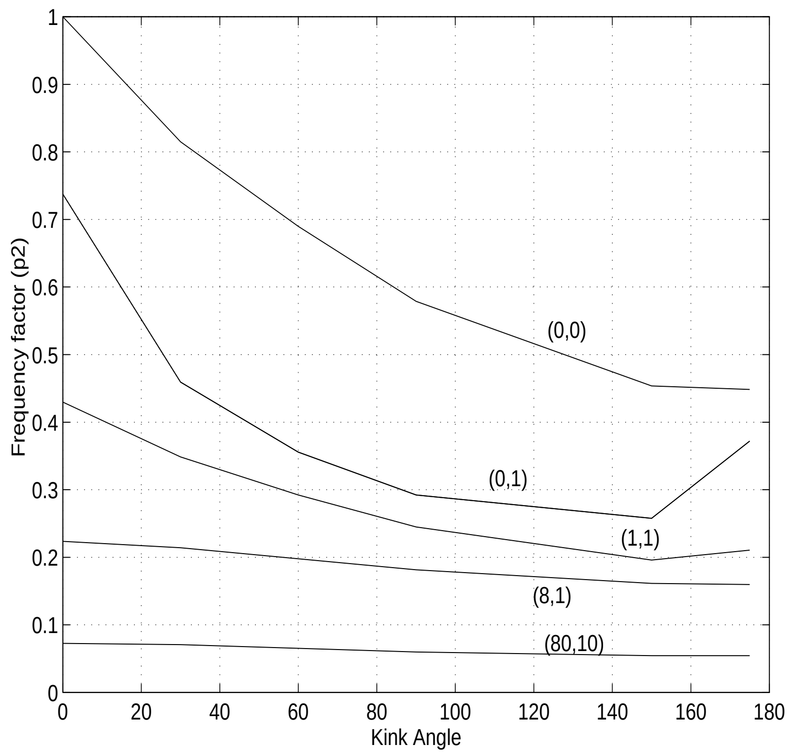

Figure 5: Mode 2 frequency factor vs Kink angle (δ) for different (m_k, m_t)

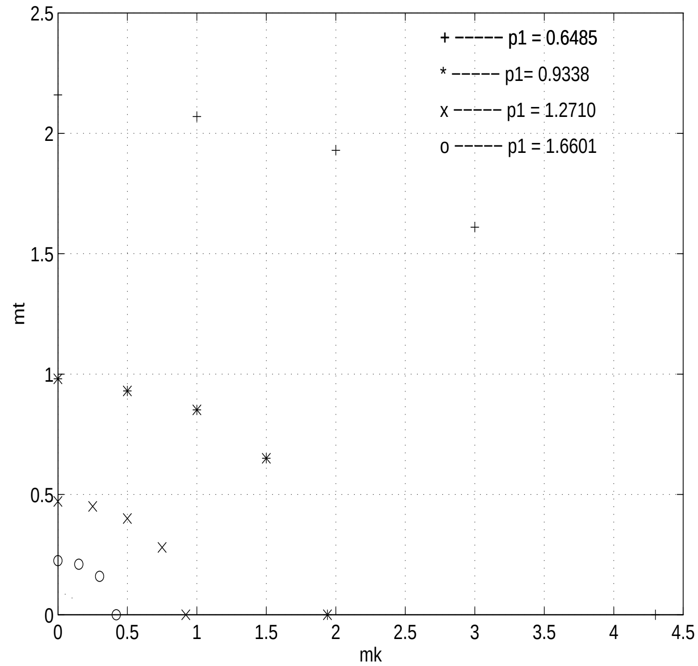

Figure 6: Iso-frequency chart for a 175° kink

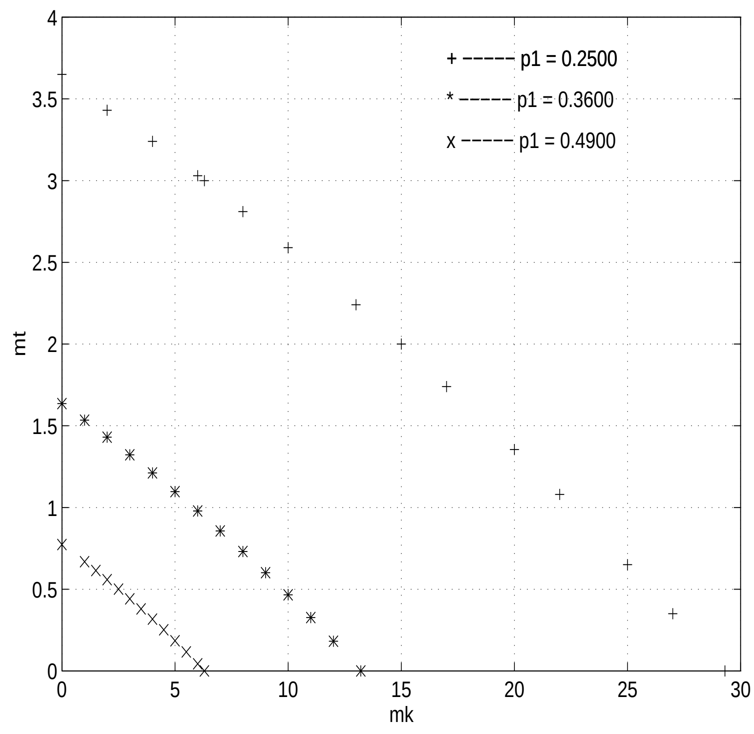

Figure 7: Iso-frequency chart for a 0° kink

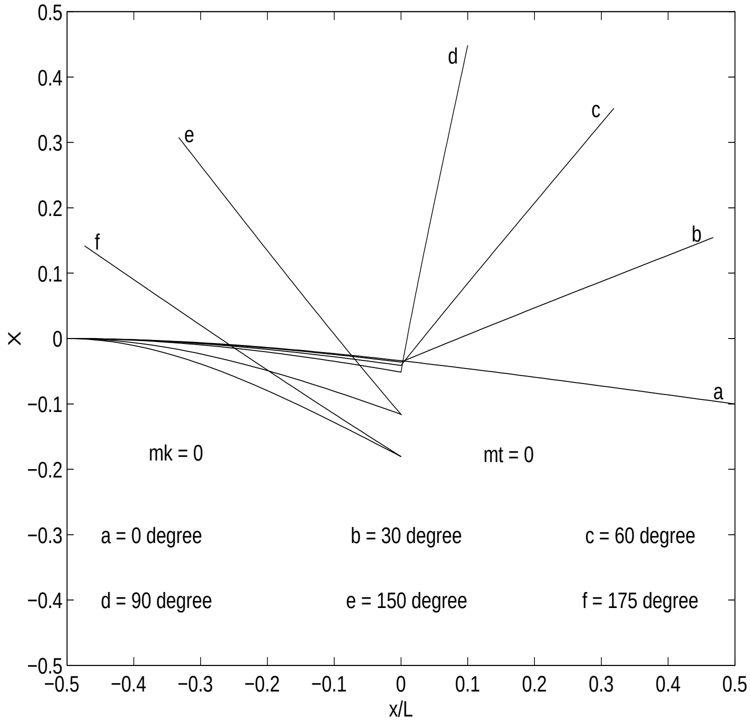

Figure 8: Mode 1 for $m_k = m_t = 0$

indicated by a negative sign for the amplitude ratios presented in Table 4.

The ratio of bending displacements at the tip (w_t) and at the kink (w_k) presented in Table 4 decreases with increasing kink angle, and for kink angles larger than 90°, deviations from this trend are noted. There is a good agreement between analytical results and results obtained from FEM, and it can be observed that for large values of m_k or m_t, the kinked cantilever beam can be reasonably approximated by a discrete model as described in section 2.

The ratio of w_k to w_t is important in controlling the vibrations of flexible robots. As an example, consider a 2-link flexible manipulator that delivers a payload to its destination at a velocity of v_t with a kink angle of 60°. Assuming $m_k = 8$ and $m_t = 1$, the frequencies are $\omega_1 = 1.278 rad/sec$ and $\omega_2 = 4.35 rad/sec$ for a beam of unit length. Let A_{1t} and A_{2t} be the amplitudes of resulting free vibrations at the tip in mode 1 and mode 2, respectively. Assuming the velocity at the kink be v_k, it is possible to use Table 4 to adjust the velocities v_t and v_k such that the amplitude of free vibration at the tip is minimum. Theoretically it is possible to achieve a zero amplitude of free vibration at the tip. Of course, in this example only the first two modes of vibrations are assumed to be excited. In the general problem the above assumption may not hold, and higher order modes may also be required to predict correct response of the kinked beam.

Table 2: MODE SHAPE COEFFICIENTS FOR MODE 1

δ	m_k	m_t	C_1	C_2	C_3	C_4	C_5	C_6	C_7	C_8
0^o	0	0	1	-0.7341	-1	0.7341	1	-0.7341	-1	0.7341
	0	1	1	-0.8650	-1	0.8650	0.9999	-0.8649	-0.9999	0.8648
	1	1	1	-0.9678	-1	0.9678	0.8945	-0.8173	-0.8805	0.7485
	8	1	1	-1.4340	-1	1.4340	0.5032	-0.6146	-0.4515	0.3298
	80	10	1	-2.5144	-1	2.5144	0.4307	-0.7665	-0.4116	0.5842
30^0	0	0	1	-0.7617	-1	0.7617	0.9609	-0.6772	-0.8445	0.5929
	0	1	1	-0.8791	-1	0.8791	0.9913	-0.8305	-0.9442	0.8111
	1	1	1	-0.9830	-1	0.9830	0.8842	-0.7841	-0.8256	0.6956
	8	1	1	-1.4479	-1	1.4479	0.4947	-0.5896	-0.4108	0.2909
	80	10	1	-2.5329	-1	2.5329	0.4181	-0.7373	-0.3884	0.5487
60^o	0	0	1	-0.7195	-1	0.7195	1.0578	-0.5336	-0.6513	0.4204
	0	1	1	-0.7671	-1	0.7671	1.1352	-0.7934	-0.9624	0.8299
	1	1	1	-0.8981	-1	0.8981	0.9867	-0.7408	-0.8059	0.6778
	8	1	1	-1.4294	-1	1.4294	0.5081	-0.5399	-0.3318	0.2157
	80	10	1	-2.5074	-1	2.5074	0.4084	-0.6854	-0.3484	0.4842
90^o	0	0	1	-0.6594	-1	0.6594	1.1884	-0.2516	-0.2295	0.0324
	0	1	1	-0.5390	-1	0.5390	1.4601	-0.7247	-1.0606	0.9251
	1	1	1	-0.7452	-1	0.7452	1.1896	-0.6598	-0.7915	0.6644
	8	1	1	-1.4116	-1	1.4116	0.5163	-0.4579	-0.1951	0.0848
	80	10	1	-2.4846	-1	2.4846	0.3843	-0.5985	-0.2776	0.3739
150^o	0	0	1	-0.7208	-1	0.7208	0.8453	0.4882	2.0752	-2.1691
	0	1	1	1.4715	-1	-1.4715	4.9379	-0.5271	-3.8153	3.5671
	1	1	1	-0.1647	-1	0.1647	2.1385	-0.3559	-1.0582	0.9145
	8	1	1	-1.4459	-1	1.4459	0.4539	-0.2598	0.1737	-0.2713
	80	10	1	-2.5328	-1	2.5328	0.2798	-0.3742	-0.0771	0.0800
175^o	0	0	1	-0.7596	-1	0.7596	0.4897	0.7074	3.6960	-2.1691
	0	1	1	26.8455	-1	-26.8455	49.8275	-2.3398	-48.4828	46.5149
	1	1	1	1.0607	-1	-1.0607	4.2824	-0.3376	-2.9800	2.7592
	8	1	1	-1.4391	-1	1.4391	0.4453	-0.2240	0.2485	-0.3438
	80	10	1	-2.5250	-1	2.5250	0.2622	-0.3368	-0.0402	0.0277

Table 3: MODE SHAPE COEFFICIENTS FOR MODE 2

δ	m_k	m_t	C_1	C_2	C_3	C_4	C_5	C_6	C_7	C_8
0^o	0	0	1	-1.0185	-1	1.0185	1	-1.0185	-0.9997	1.0181
	0	1	1	-1.0060	-1	1.0060	0.9999	-1.0061	-0.9998	1.0058
	1	1	1	-1.2857	-1	1.2857	-0.2806	-1.2444	1.8464	-1.8358
	8	1	1	-1.9881	-1	1.9881	-1.6194	-0.6874	2.9547	-2.9305
	80	10	1	-3.4869	-1	3.4869	-2.1743	0.8403	2.6279	-2.9910
30^0	0	0	1	-1.0985	-1	1.0985	0.3995	-1.3732	2.0224	-1.9933
	0	1	1	-1.2262	-1	1.2262	-0.1308	-1.1886	1.8176	-1.8088
	1	1	1	-1.4239	-1	1.4239	-0.6603	-1.0697	2.2806	-2.2694
	8	1	1	-2.0519	-1	2.0519	-1.6951	-0.6050	3.0424	-3.0173
	80	10	1	-3.5849	-1	3.5849	-2.2148	0.9225	2.6697	-3.0573
60^o	0	0	1	-1.1627	-1	1.1627	-0.1461	-1.3411	3.8169	-3.7784
	0	1	1	-1.3512	-1	1.3512	-0.5302	-0.9013	2.4185	-2.4120
	1	1	1	-1.5309	-1	1.5309	-0.8641	-0.7959	2.5424	-2.5339
	8	1	1	-2.1543	-1	2.1543	-1.7940	-0.4477	3.1800	-3.1544
	80	10	1	-3.7572	-1	3.7572	-2.2704	1.0711	2.7337	-3.1672
90^o	0	0	1	-1.2378	-1	1.2378	-0.6265	-1.1328	4.9242	-4.8734
	0	1	1	-1.4221	-1	1.4221	-0.6437	-0.5666	2.6044	-2.6046
	1	1	1	-1.6177	-1	1.6177	-0.9351	-0.5013	2.6453	-2.6425
	8	1	1	-2.3014	-1	2.3014	-1.9401	-0.2666	3.3715	-3.3437
	80	10	1	-4.0067	-1	4.0067	-2.3806	1.2752	2.8560	-3.3549
150^o	0	0	1	-1.5685	-1	1.5685	-1.6262	-1.1656	6.1934	-6.0757
	0	1	1	-1.2433	-1	1.2433	-0.1887	-0.0395	2.5244	-2.5477
	1	1	1	-1.6044	-1	1.6044	-0.6750	-0.0994	2.4487	-2.4648
	8	1	1	-2.6869	-1	2.6869	-2.4504	-0.0289	3.9407	-3.8969
	80	10	1	-4.6274	-1	4.6274	-2.8291	1.7450	3.3223	-3.9719
175^o	0	0	1	-1.8783	-1	1.8783	-2.4117	-1.8136	7.0139	-6.8313
	0	1	1	-0.9772	-1	0.9772	0.0574	0.2764	3.6476	-3.6691
	1	1	1	-1.3826	-1	1.3826	-0.2979	-0.0179	2.2831	-2.3104
	8	1	1	-2.7589	-1	2.7589	-2.5616	-0.0060	4.0570	-4.0093
	80	10	1	-4.7415	-1	4.7415	-2.9298	1.8284	3.4246	-4.1005

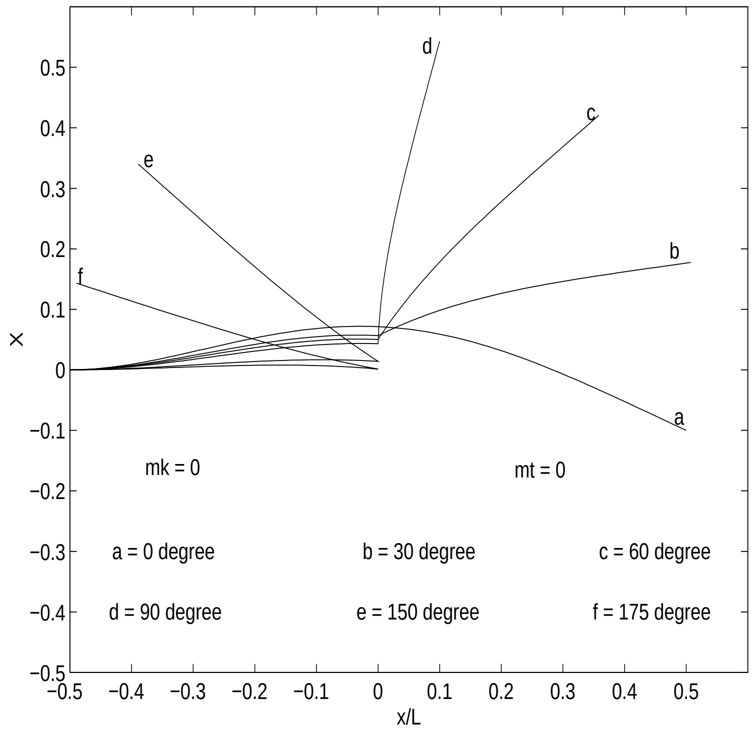

Figure 9: Mode 2 for $m_k = m_t = 0$

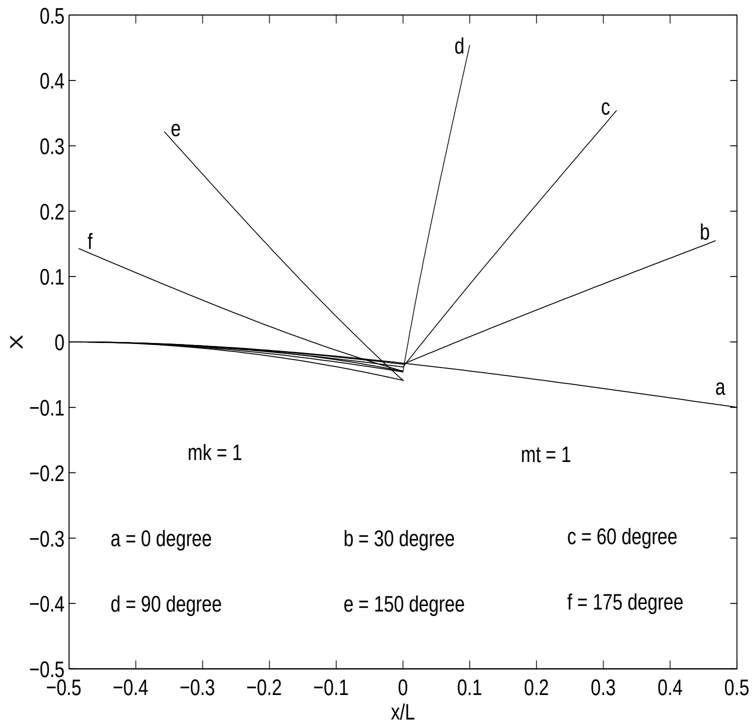

Figure 10: Mode 1 for $m_k = m_t = 1$

Table 4: VIBRATION AMPLITUDE RATIO

			MODE 1	MODE 1	MODE 2	MODE 2
m_k	m_t	δ	ANALYTICAL	FEM	ANALYTICAL	FEM
0	0	0^o	2.9453	2.9497	-1.4012	-1.3777
0	1	-	3.1494	3.1488	-0.2093	-0.2070
1	1	-	3.0878	3.0885	-0.4799	-0.4769
8	1	-	2.8419	2.8425	-2.6178	-2.6085
80	10	-	2.8299	2.8300	-2.8034	-2.8000
0	0	30^o	2.7819	2.8184	-1.7700	-1.4938
0	1	-	3.0008	3.0301	-0.3940	-0.3264
1	1	-	2.9387	2.9624	-0.6910	-0.5976
8	1	-	2.6938	2.7036	-2.9717	-2.8485
80	10	-	2.6834	2.6906	-3.1472	-3.0568
0	0	60^o	2.4288	2.4599	-1.9910	-1.8095
0	1	-	2.6890	2.7142	-0.5403	-0.5204
1	1	-	2.6061	2.6275	-0.8870	-0.8508
8	1	-	2.3121	2.3208	-3.6031	-3.5403
80	10	-	2.3002	2.3068	-3.8265	-3.7940
0	0	90^o	1.9483	1.9717	-2.3143	-2.2273
0	1	-	2.3206	2.3366	-0.6319	-0.6575
1	1	-	2.1798	2.4078	-1.0734	-1.0854
8	1	-	1.7799	1.7869	-4.7490	-4.7148
80	10	-	1.7668	1.7722	-5.0571	-5.0519
0	0	150^o	0.8629	1.1705	-7.1548	-2.6714
0	1	-	2.5030	2.8752	-0.3017	-0.1662
1	1	-	1.7019	1.9521	-1.0045	-0.8056
8	1	-	0.7895	0.8015	-10.6223	-9.8592
80	10	-	0.7873	0.7949	-10.7502	-10.2860
0	0	175^o	0.5540	1.3360	-74.3250	-1.5727
0	1	-	3.7362	3.8643	-0.03610	-0.0231
1	1	-	2.2342	2.3500	-0.5075	-0.4419
8	1	-	0.6362	0.6512	-12.7434	-12.3061
80	10	-	0.6362	0.6381	-12.6762	-12.5252

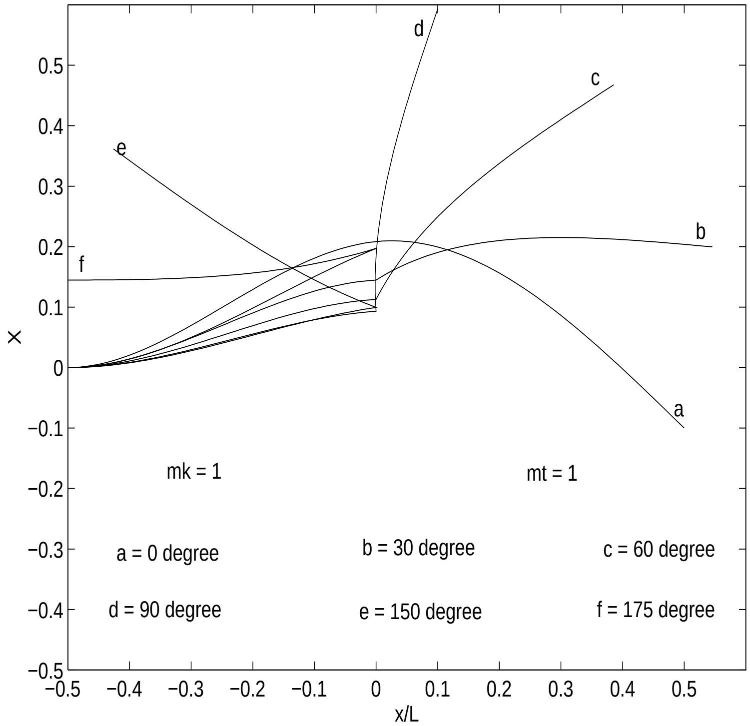

Figure 11: Mode 2 for $m_k = m_t = 1$

Bending Moments

The static bending moment at the support can be calculated using equation (16). The dynamic moment per unit tip deflection is given by $3(EI/L^2)D_s$. Hence the ratio of dynamic to static bending moment can be calculated for any particular configuration. It may be noted that this ratio becomes infinite for $\delta = \pi$, even though the dynamic moment remains finite, equal to $3(EI/L^2)D_s$. Multiplying the dynamic moment at the support by D_k gives the dynamic moment at the kink. The dynamic moment at the support for a straight beam in mode 1 is shown in Figure 12. The kink mass, m_k is varied between 0 and 80. The tip mass, m_t is varied between 0 and 10. The 3-D surface has a maximum elevation of 1.6 for $m_k = 80$ and $m_t = 0$ i.e. for negligible tip mass. When the kink mass becomes negligible, the dynamic factor becomes unity for $m_t = 10$ and $m_k = 0$ along the axis of $m_k = 0$. The dynamic factor increases from its unit value for large m_t to a maximum value of 1.17 for $m_k = m_t = 0$ corresponding to a straight beam without attached masses. This particular value of $D_s = 1.17$ is obtained for a fixed ratio of $\frac{m_k}{m_t} = 3.8$. For this particular mass ratio, therefore, the dynamic moment at the support is invariant as shown by the line AB.

The above observation can be partially explained using the discrete model outlined in section 2. According to equation (22), the dynamic moment per unit tip deflection is an explicit function of the mass ratio ($\frac{m_k}{m_t}$), and, for $\frac{m_k}{m_t} = 3.8$, there is no change in M_s. For mass ratios greater than

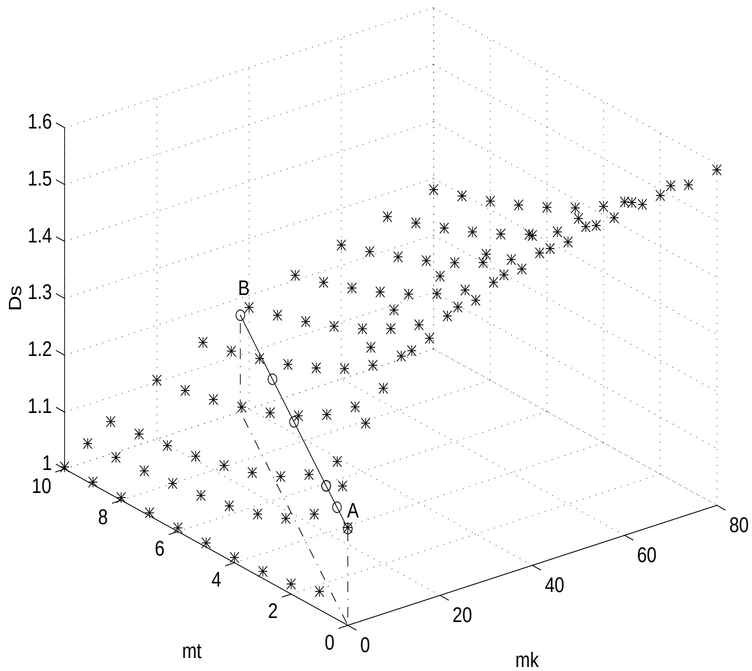

Figure 12: Dynamic moment for straight beam in mode 1

3.8, the dynamic moment factor increases towards the maximum value of 1.6 depending on the value of m_k. For mass ratios less than 3.8, the dynamic factor decreases towards the minimum value of 1 as shown.

Table 5 gives the bending moments at the kink and at the support. This information is useful to design the cross sectional dimensions of the links of a flexible manipulator once the tip displacement is specified. In general, the bending moment at the support is more than that at the kink in mode 1. However, as the kink angle becomes more than $\pi/2$, there is a reversal in the trend for small values of m_k and m_t. Eventually at $\delta = \pi$, the bending moment at the kink becomes many times larger than the value at the support.

5 Conclusion

This paper deals with the free vibration characteristics of a kinked cantilever beam carrying discrete masses. Euler beam theory is used to obtain natural frequencies, mode shapes and static and dynamic bending moments. The presence of masses at the tip and kink significantly alters the natural frequencies, mode shapes and bending moments in a kinked beam. The results obtained in this paper are useful for analysis and design of control schemes for flexible manipulators, or for predicting seismic response of two-storied structures. In particular, the dynamic moment factors

Table 5: BENDING MOMENTS

			MODE 1	MODE 1	MODE 1	MODE2	MODE 2	MODE 2
m_k	m_t	δ	$\hat{M}_{dyn}$	D_s	D_k	$\hat{M}_{dyn}$	D_s	D_k
0	0	0^o	-3.5160	-1.1720	0.3395	22.0334	7.3445	-0.7137
0	1	-	-3.0965	-1.0322	0.4659	107.1191	35.7064	-0.6137
1	1	-	-3.2262	-1.0754	0.4132	47.3841	15.7947	-0.8364
8	1	-	-3.8057	-1.2686	0.2215	11.4306	3.8102	-1.1712
80	10	-	-3.8402	-1.2801	0.2087	10.7814	3.5938	-1.2031
0	0	30^o	-3.7648	-1.2549	-0.3134	17.2794	5.7598	-0.8713
0	1	-	-3.2659	-1.0886	-0.4534	56.0590	18.6863	-0.7881
1	1	-	-3.4085	-1.1362	-0.4002	33.1692	11.0564	-0.8816
8	1	-	-4.0335	-1.3445	-0.2113	10.3283	3.4428	-1.1939
80	10	-	-4.0661	-1.3554	-0.1999	9.8329	3.2776	-1.2219
0	0	60^o	-4.3044	-1.4348	-0.3227	14.7938	4.9313	-0.9339
0	1	-	-3.5771	-1.1924	-0.5007	39.2978	13.0993	-0.7930
1	1	-	-3.8013	-1.2671	-0.4277	25.1528	8.3843	-0.8740
8	1	-	-4.7241	-1.5747	-0.2000	8.7789	2.9263	-1.2208
80	10	-	-4.7690	-1.5897	-0.1881	8.3690	2.7897	-1.2483
0	0	90^o	-5.3640	-1.7880	-0.3353	12.2433	4.0811	-0.9726
0	1	-	-5.1032	-1.7011	-0.3463	31.2866	10.4289	-0.7331
1	1	-	-4.4333	-1.4778	-0.4905	19.7541	6.5847	-0.8340
8	1	-	-6.2030	-2.0677	-0.1770	7.1373	2.3791	-1.2751
80	10	-	-6.2742	-2.0914	-0.1654	6.8291	2.2764	-1.3032
0	0	150^o	-13.4840	-4.4947	-0.1460	6.0608	2.0203	-1.3482
0	1	-	-2.2366	-0.7455	-2.3108	51.8472	17.2824	-0.4202
1	1	-	-4.9191	-1.6397	-0.8821	17.8500	5.9500	-0.6364
8	1	-	-14.5509	-4.8503	-0.0933	4.8344	1.6115	-1.5205
80	10	-	-14.5771	-4.8590	-0.0916	4.7550	1.5850	-1.5292
0	0	175^o	-22.9307	-7.6436	-0.0205	4.0924	1.3641	-1.8459
0	1	-	-0.2359	-0.0786	-25.3771	408.9152	136.3051	-1.8459
1	1	-	-2.7272	-0.9091	-1.9628	31.1179	10.3726	-0.4496
8	1	-	-18.1914	-6.0638	-0.0784	4.5742	1.5247	-1.5767
80	10	-	-18.1526	-6.0509	-0.0786	4.5192	1.5064	-1.5797

provide useful guidelines in design for practical problems. Similar analysis can be extended to composite beams or multi-link configurations. Finally, this paper highlights the utility of a simple discrete model of a kinked cantilever model which leads to a better understanding of the results obtained from numerical and analytical models.

ACKNOWLEDGMENTS

We thank Department of Space and Department of Science and Technology, Govt. of India for supporting this work.

References

[1] K. F. Graff, *Wave Motion in Elastic Solids*, Clarendon Press, 1975.

[2] R. W. Clough, and J. Penzien, *Dynamics of Structures*, McGraw-Hill, New York, 1993.

[3] A. K. Chopra, *Dynamics of Structures, Theory and Applications to Earthquake Engineering*, PHI Pvt. Ltd, 1996.

[4] P. A. A. Laura, J. L. Pombo and E. A. Susemihl, "A Note on the Vibrations of a Clamped-Free Beam with a Mass at the Free End," *Journal of Sound and Vibration*, Vol. 37, No. 2, pp. 161-168, 1974.

[5] H. Abramovich and O. Hamburger, " A Vibration of a Cantilever Timoshenko Beam with a Tip Mass," *Journal of Sound and Vibration*, Vol. 148, No. 1, pp. 162-170, 1991.

[6] H. H. Pan, "Transverse Vibration of an Euler Beam Carrying a System of Heavy Bodies," *Journal of Applied Mechanics*, Vol. 32, pp. 434-437, 1965.

[7] Luo, Z. H., "Direct Strain Feedback Control of Flexible Robot Arms: New Theoretical and Experimental Results," *IEEE Transactions on Automatic Control*, Vol. AC-38, No. 11, pp. 1610-1622, 1993.

[8] Johnson W, *Impact Strength of Materials*, Edward Arnold Ltd., 1972.

[9] C. M. Harris, *HandBook of Acoustical Measurements and Noise Control*, Chapter 27, McGraw-Hill, Third Edition, 1991.

[10] *Matlab Users Manual*, The MathWorks, Inc.

Appendix: Elements of the 8x8 matrix F(KL) in eqn(8)

$a(1,1) = 1; a(1,2) = 0; a(1,3) = 1; a(1,4) = 0; a(1,5) = a(1,6) = 0; a(1,7) = a(1,8) = 0; a(2,1) = 0; a(2,2) = 1; a(2,3) = 0; a(2,4) = 1; a(2,5) = 0; a(2,6) = 0; a(2,7) = 0; a(2,8) = 0; a(2,8) = 0; a(3,1) = \cos(0.5 * y_j) * \cos(\delta); a(3,2) = \sin(0.5 * y_j) * \cos(\delta); a(3,3) = \cosh(0.5 * y_j) * \cos(\delta); a(3,4) = \sinh(0.5 * y_j) * \cos(\delta); a(3,5) = -\cos(0.5 * y_j); a(3,6) = -\sin(0.5 * y_j); a(3,7) = -\cosh(0.5 * y_j); a(3,8) = -\sinh(0.5 * y_j); a(4,1) = -\sin(0.5 * y_j); a(4,2) = \cos(0.5 * y_j); a(4,3) = \sinh(0.5 * y_j); a(4,4) = \cosh(0.5 * y_j); a(4,5) = \sin(0.5 * y_j); a(4,6) = -\cos(0.5 * y_j); a(4,7) = -\sinh(0.5 * y_j); a(4,8) = -\cosh(0.5 * y_j); a(5,1) = -\cos(0.5 * y_j); a(5,2) = -\sin(0.5 * y_j); a(5,3) = \cosh(0.5 * y_j); a(5,4) = \sinh(0.5 * y_j); a(5,5) = \cos(0.5 * y_j); a(5,6) = \sin(0.5 * y_j); a(5,7) = -\cosh(0.5 * y_j); a(5,8) = -\sinh(0.5 * y_j); a(6,1) = \sin(0.5 * y_j) + m_{ek} * y_j * \cos(0.5 * y_j); a(6,2) = -\cos(0.5 * y_j) + m_{ek} * y_j * \sin(0.5 * y_j); a(6,3) = \sinh(0.5 * y_j) + m_{ek} * y_j * \cosh(0.5 * y_j); a(6,4) = \cosh(0.5 * Y) + m_{ek} * y_j * \sinh(0.5 * y_j); a(6,5) = -\sin(0.5 * y_j) * \cos(\delta); a(6,6) = \cos(0.5 * y_j) * \cos(\delta); a(6,7) = -\sinh(0.5 * y_j) * \cos(\delta); a(6,8) = -\cosh(0.5 * y_j) * \cos(\delta); a(7,1) = 0; a(7,2) = 0; a(7,3) = 0; a(7,4) = 0; a(7,5) = \cos(y_j); a(7,6) = \sin(y_j); a(7,7) = -\cosh(y_j); a(7,8) = -\sinh(y_j); a(8,1) = 0; a(8,2) = 0; a(8,3) = 0; a(8,4) = 0; a(8,5) = \sin(y_j) + m_{et} * y_j * \cos(y_j); a(8,6) = -\cos(y_j) + m_{et} * y_j * \sin(y_j); a(8,7) = \sinh(y_j) + m_{et} * y_j * \cosh(y_j); a(8,8) = \cosh(y_j) + m_{et} * y_j * \sinh(y_j);$